Biochemical and Biophysical Research Communications 453 (2014) 449–454

Contents lists available at ScienceDirect

Biochemical and Biophysical Research Communications

journal homepage: www.elsevier.com/locate/ybbrc

Design of non-aggregating variants of Aβ peptide

Joanne M. Caine [a,b,c,*], Quentin Churches [a,b], Lynne Waddington [a,b], Julie Nigro [a,b,c], Kerry Breheney [a,b,c], Colin L. Masters [c,d], Stewart D. Nuttall [a,b,c], Victor A. Streltsov [a,b,c,*]

[a] CSIRO Materials Science and Engineering, 343 Royal Parade, Parkville, Victoria 3052, Australia
[b] Preventative Health Flagship, 343 Royal Parade, Parkville, Victoria 3052, Australia
[c] CRC for Mental Health, Level 2, 161 Barry Street, Carlton South, Victoria 3053, Australia
[d] Florey Institute for Neuroscience and Mental Health, 30 Royal Parade, Parkville, Victoria 3052, Australia

ARTICLE INFO

Article history:
Received 18 September 2014
Available online 1 October 2014

Keywords:
Amyloid beta
Alzheimer's disease
Non-aggregating mutations

ABSTRACT

Self association of the amyloid-β ($A\beta_{42}$) peptide into oligomers, high molecular weight forms, fibrils and ultimately neuritic plaques, has been correlated with progressive cognitive decline in Alzheimer's disease. Thus, insights into the drivers of the aggregation pathway have the capacity to significantly contribute to our understanding of disease mechanism. Functional assays and a three-dimensional crystal structure of the P3 amyloidogenic region 18–41 of Aβ were used to identify residues important in self-association and to design novel non-aggregating variants of the peptide. Biophysical studies (gel filtration, SDS–PAGE, dynamic light scattering, thioflavin T assay, and electron microscopy) demonstrate that in contrast to wild type Aβ these targeted mutations lose the ability to self-associate. Loss of aggregation also correlates with reduced neuronal toxicity. Our results highlight residues and regions of the Aβ peptide important for future targeting agents aimed at the amelioration of Alzheimer's disease.

1. Introduction

One characteristic of Alzheimer's disease (AD) is the formation of extracellular fibrillar plaques composed primarily of the 42 amino acid form of amyloid-β peptide ($A\beta_{42}$), a cleavage product of the membrane bound amyloid precursor protein (APP) [1]. The pathological form of Aβ was initially believed to be the fibrillar form of the peptide but the current consensus is that soluble oligomeric Aβ forms are also toxic to neurons [2–6]. Thus, it appears that a number of intermediates along the aggregation pathway may be important to Aβ mediated neuronal cell dysfunction leading to acute memory loss in Alzheimer's disease.

Studies using synthesised Aβ showed that both the hydrophilic metal binding N-terminus and the hydrophobic fibrillogenic C-terminus play important roles in overall Aβ toxicity [7–9]. Structural information of the Aβ oligomers has been limited due to the aggregative nature of the peptide however, some partial structures have been obtained by NMR and crystallography of fusions of the Aβ peptide with other proteins [10–16]. Further information on important residues inhibiting the formation of oligomers and/or fibrils has been obtained by mutation studies [17].

The crystal structure of the Aβ fragment 18–41 fused to a shark antibody (IgNAR) protein [10], showed that the β-hairpins (32–41) from four chains of Aβ form the hydrophobic core of the tetramer. Further docking studies using this tetrameric model have explored the binding of aggregation inhibitors to oligomeric Aβ [18]. Molecular dynamics simulations [19] have shown that this $A\beta_{18-41}$ tetramer was more stable with increased length ($A\beta_{17-43}$) and with the β-strands (G33-M35 and V39-A42) connected by the turn V36-G38 forming the most stable parts of the structure. On the other hand, the inhibition of aggregation with peptide $M_{35}VGGV_{39}$ [20] indicated that the region comprising G33 to V39 is critical for aggregation and binding of Aβ to neuronal cells. Another cell viability screen [21] identified $A\beta_{31-42}$ and $A\beta_{39-42}$ as the most potent inhibitors. Biophysical characterisation [21] indicated that the action of these peptides likely involved stabilisation of $A\beta_{42}$ into nontoxic oligomers. Therefore, in this study we focused on the region 32–42 to design mutations in $A\beta_{42}$ peptide that would inhibit aggregation of the monomeric form and/or stabilise the tetramer in nontoxic form. To help define the mechanisms of Aβ-mediated aggregation and toxicity, we compare wild type peptide with two designed variants, and another peptide with

Abbreviations: Aβ, amyloid-β peptide; AD, Alzheimer's disease; wt, wild type; NGF, nerve-growth factor; ThT, thioflavin T.

* Corresponding authors at: CSIRO Manufacturing Flagship, 343 Royal Parade, Parkville, Victoria 3052, Australia.

E-mail addresses: jo.caine@csiro.au (J.M. Caine), victor.streltsov@csiro.au (V.A. Streltsov).

http://dx.doi.org/10.1016/j.bbrc.2014.09.102
0006-291X/

mutations at position 19 and 34 (F19S: L34P) which was shown to have superior non-aggregating properties [17].

2. Materials

Human $A\beta_{1-42}$ wild type ($A\beta_{42}$) and its mutants were synthesised and purified by Dr. James I. Elliott (Yale University, New Haven, CT) and verified by mass spectrometry (MS). Analytical grade ammonium hydroxide (NH_4OH) (28% v/v) was from Sigma Chemical Co. (St. Louis, MO). Poly-L-lysine coated 96-well plates were from BD (Franklin Lakes, NJ Cat. No. 356516). The F12K media, horse serum, penicillin, streptomycin, amphotericin B, trypsin/EDTA and human recombinant β-nerve growth factor (NGF) were from Invitrogen (Grand Island, NY). Foetal bovine serum (FBS) was from SAFC Biosciences (Lenexa, KS). Cytotoxicity detection kit (lactate dehydrogenase) was from Roche Diagnostics (Mannheim, Germany). All reagents otherwise not indicated were of analytical grade.

3. Methods

3.1. Structure-based peptide design mutations

Mutants $A\beta_{42}$TTAN and $A\beta_{42}$NRET were designed based on the $A\beta_{18-41}$ tetramer structure (PDB 3MOQ) [10] visualised using PyMol [22] (Fig. 1A), together with residues showing highest increase of fluorescence in random mutations of GFP-$A\beta_{42}$ fusion [17]. We identified key hydrophobic residues at positions 19, 32, 34, 35, 39 and 41 as important in oligomer and amyloid formation (Fig. 1A). F19 is an important residue for stabilising the dimer since its phenyl ring is inserted to the hydrophobic pocket formed by residues across the dimer interface [10]. The mutation F19**S** combined with the L34**P** mutation in the hydrophobic core of the tetramer (Fig. 1A and [10]) has been reported to compromise significantly (up to 100%) the $A\beta_{42}$ aggregation [17]. Sidechains of I32, M35, V39 and I41 residues are solvent exposed on the tetramer surface (Fig. 1A) and likely to interact with next subunit forming tetramer-tetramer interface. When those residues were mutated to **TTAN** (I32**T**, M35**T**, V39**A**, I41**N**) or to **NRET** (I32**N**, M35**R**, V39**E**, I41**T**) the GFP-$A\beta_{42}$ fluorescence [17] was increased over 75% and between 40% and 70% for each set of mutations, correspondently [17]. Further, $A\beta_{42}$TTAN and $A\beta_{42}$NRET mutants were compared with $A\beta_{42}$SP in biophysical experiments.

3.2. Peptide pre-treatment with NH_4OH

Peptides were dissolved in 10% (w/v) NH_4OH to 1 mg/ml, lyophilised and stored as previously described [23]. Prior to experiments, NH_4OH treated and untreated $A\beta_{42}$ were dissolved in 60 mM NaOH or DMSO and concentrations determined by absorbance at 214 and 280 nm using extinction coefficients of 76848 M^{-1} cm^{-1} or 1490 M^{-1} cm^{-1}, respectively. All resuspended peptides were analysed by MS which indicated the peptide to be unmodified. Circular dichroism (CD) validation showed identical spectra at $t = 0$ (Supplementary Fig. S1). Samples were taken for gel electrophoresis analysis.

All experimental results are $n = 2$ or more unless otherwise stated. All peptides were pre-treated and dissolved in NaOH or DMSO for consistency (the three mutants had a higher solubility in aqueous solutions that the wild type $A\beta_{42}$). Characterisation of the mutants dissolved directly in water gave similar results to NH_4OH/NaOH treatment (data not shown).

3.3. Dynamic light scattering (DLS)

The method for DLS was as previously described [23]. All peptides were dissolved in DMSO and diluted to a final concentration of 100 μM in 50 mM Tris pH8/10 mM EDTA. A separate aliquot of $A\beta_{42}$SP was dissolved in 60 mM NaOH before dilution.

3.4. Thioflavin T assays (ThT)

The method for ThT assays was as previously described [24] with minor modifications. Briefly, peptides were dissolved in

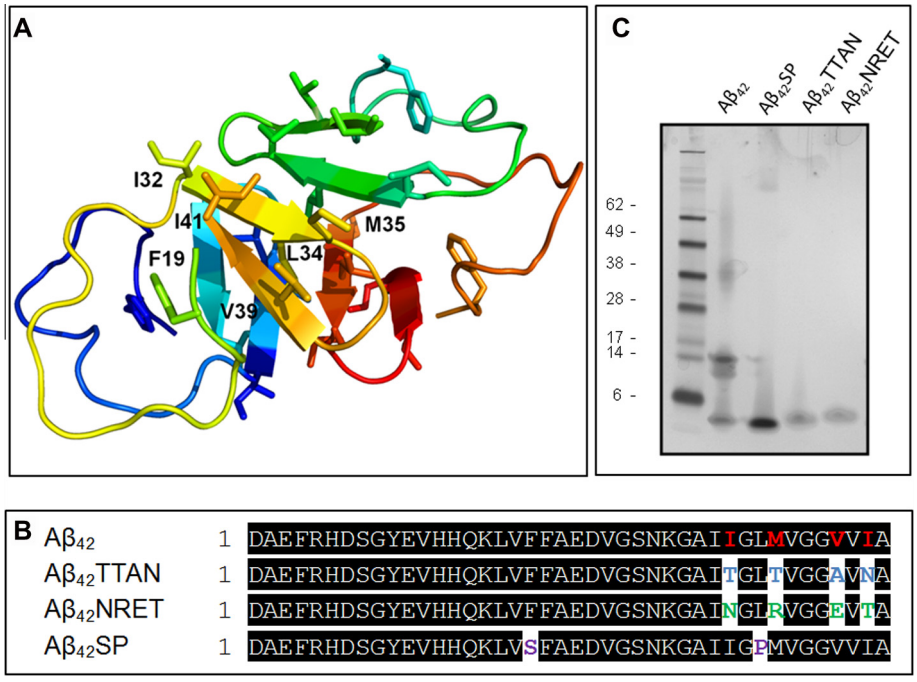

Fig. 1. Structure, PAGE and alignment of Aβ peptide and its mutants. (A) Crystal structure of $A\beta_{18-41}$ tetramer from Aβ-IgNAR fusion [10] highlighting residues targeted for mutation. (B) Sequence alignment of $A\beta_{42}$ and variants $A\beta_{42}$TTAN, $A\beta_{42}$NRET, and $A\beta_{42}$SP. (C) The gel was visualised with silver staining.

60 mM NaOH or DMSO (stock concentration of 1–2 mM) and diluted to 20 μM in 50 mM KH_2PO_4/150 mM NaCl pH7.4 in a 96 well plate (total volume = 200 μl). Vehicle controls of 60 mM NaOH were shown not to alter the pH of the final solution. The plate was incubated at 37 °C without agitation. At $t = 0$ and two or more later time-points (up to 48 h), peptides were sampled (20 μl) and added to a 96 well solid black plate containing ThT (2 μM in 50 mM glycine pH8.5, freshly diluted from a 500 μM frozen stock). The plate was incubated 15 min at room temperature in the dark. The ThT fluorescence was recorded using 440 nm and 485 nm excitation and emission filters, respectively in a FLUOstar Optima (BMG LABTECH, Germany) plate reader.

3.5. Transmission electron microscopy (TEM)

Peptide samples were prepared as for ThT assay (20 μM in 50 mM KH_2PO_4/150 mM NaCl pH7.4) in screw top 1.5 ml microtubes and incubated at 37 °C (without shaking) for 30 days. The samples were gently agitated before taking an aliquot to image by negative stain TEM as previously described [18].

3.6. Neuronal cell model and cytotoxicity assay

NGF-differentiated rat pheochromocytoma (PC)-12 cultures were cultured and plated as previously described [23]. The NH_4OH pre-treated peptides (0.5 mg) were reconstituted as previously described [25]. A vehicle control was prepared in an identical manner and the supernatants were collected and measured for absorbance at 214 nm. The peptide concentration was determined using the theoretical molar extinction coefficient ($A\beta_{42}$ 76848 $M^{-1}\,cm^{-1}$, $A\beta_{42}$TTAN 75985 $M^{-1}\,cm^{-1}$, $A\beta_{42}$NRET 76133 $M^{-1}\,cm^{-1}$ and $A\beta_{42}$SP 74312 $M^{-1}\,cm^{-1}$) [26]. All peptides were diluted to 200 μM with vehicle buffer and subsequently diluted to 15 μM in culture medium (F12K, 0.5% foetal calf serum, 100 ng/ml NGF, 100 U/ml penicillin G sodium, 100 μg/ml streptomycin sulfate and 0.25 μg/ml amphotericin B). Vehicle was diluted in culture medium in an identical manner. Cultures were treated with peptides and controls as previously described [25]. Cytotoxicity was assessed as previously described [25].

4. Results

4.1. Structure-based design of non-aggregating Aβ peptides mutations

Combining our structural information on the $A\beta_{17-41}$ tetramer [10] and mutations previously demonstrated to reduce aggregation [17], we identified and selected the following mutations in $A\beta_{42}$: (1) F19S; (2) I32T and I32N; (3) L34P; (4) M35T and M35R; (5) V39A and V39E; and (6) I41N and I41T (Fig. 1A). Mutations were incorporated into three peptides (Fig. 1B) termed $A\beta_{42}$TTAN, which incorporated the mutant sequence: I32**T**, M35**T**, V39**A** and I41**N**; $A\beta_{42}$NRET, which incorporated a second set of mutations: I32**N**, M35**R**, V39**E** and I41**T**; and the previously reported peptide $A\beta_{42}$SP which incorporated both F19**S** and L34**P** [17]. We hypothesised that these mutations would significantly reduce the self-aggregation properties of the $A\beta_{42}$ peptide.

4.2. Peptide preparation and characterisation

The wt $A\beta_{42}$ and three variant peptides were synthesised and pre-treated according to our recently described NH_4OH preparation protocol which results in dissociation to monomeric form [23]. Following resuspension in 60 mM NaOH or DMSO (dependent upon the subsequent experiment), peptides were validated by mass spectrometry (data not shown) and CD spectroscopy (Supplementary Fig. S1). Gel electrophoresis of peptides showed that $A\beta_{42}$ exhibited the pattern of higher molecular weight oligomers, while both $A\beta_{42}$TTAN and $A\beta_{42}$NRET migrated as predominantly monomeric species (Fig. 1C). Similarly, $A\beta_{42}$SP migrated as a predominant monomeric band with at least one higher molecular weight species (Fig. 1C). Even though equal amounts of the peptides were loaded, the $A\beta_{42}$TTAN and $A\beta_{42}$NRET did not silver stain to the same degree so digital enhancement software was used to check for the presence of minor bands but none were found in these two mutants. Fig. 1 contains the unenhanced image of the gel. Similar data were obtained by gel filtration (GF, Supplementary Fig. S2). The wt and variant peptides were then compared in a series of biophysical experiments.

4.3. Dynamic light scattering (DLS) and thioflavin T (ThT) assays

For DLS, within the 20–30 min incubation time between adding the peptide to the plate and obtaining data, $A\beta_{42}$ developed a multimodal polydisperse pattern. One peak had a hydrodynamic radius (R_h) of 1.6 nm and a broad peak with a R_h of 4–11 nm (Fig. 2A). This is consistent with our previous $A\beta_{42}$ profiles [23]. In contrast, both $A\beta_{42}$TTAN and $A\beta_{42}$NRET were present as single peaks (Fig. 2A): for $A\beta_{42}$TTAN this presents as a broad polydisperse peak with a R_h range of 0.9–2.0 nm, while $A\beta_{42}$NRET is present as a single narrow peak with a ~1.5 nm R_h radius. For $A\beta_{42}$SP there was some discrepancy between samples prepared in DMSO, which showed a monomodal monodisperse peak with a R_h of 3.0 nm, and samples prepared in NaOH, which showed a multimodal polydisperse result with one peak also with a R_h of 3.0 nm but a further peak at R_h = 4.2 nm (Fig. 2B). In contrast, no discrepancy was observed for $A\beta_{42}$TTAN and $A\beta_{42}$NRET between NaOH and DMSO preparations (results not shown). Thus, as our results are representative of data from a minimum of 2 separate experiments we are confident that the $A\beta_{42}$TTAN and $A\beta_{42}$NRET mutant peptides occur as predominantly stabilised small oligomeric or monomeric species in solution.

The ThT assay, a benchmark test for Aβ aggregation [27], was used to compare the rates and degree of aggregation of wt and mutant peptides. $A\beta_{42}$ prepared in NaOH had the highest aggregation rate, though when dissolved in DMSO before addition to assay buffer, aggregation was slower and failed to reach the NaOH sample fluorescent maximum (Fig. 2C and D). The same solvent effect was observed for $A\beta_{42}$SP where little aggregation occurred for peptide prepared in DMSO, while there was some aggregation observed when dissolved in NaOH. $A\beta_{42}$TTAN and $A\beta_{42}$NRET showed very little increased fluorescence compared to solvent alone control for either NaOH (Fig. 2C and D) or DMSO (results not shown). The data are representative of two independent 30 day experiments but the same non-aggregation effect of the mutants was also seen in more commonly performed 24 h ThT assays (not shown).

4.4. Transmission electron microscopy (TEM)

Electron microscopy provides a visual representation of the aggregation end-point of the ThT assay. Wild type $A\beta_{42}$ had a typical abundant fibrillar pattern (Fig. 3A). Compared with wt, $A\beta_{42}$SP dissolved in NaOH showed fewer fibrils (Fig. 3B). Consistent with the ThT assay results, $A\beta_{42}$SP prepared in DMSO resulted in few short protofibrils (Fig. 3E), whilst $A\beta_{42}$TTAN and $A\beta_{42}$NRET showed no obvious fibril formation after NaOH preparation (Fig. 3C and D respectively).

4.5. Neuronal toxicity assay

Cytotoxicity assays were used to correlate with aggregation properties. Compared with vehicle treated cultures (1.4 ± 1.1%

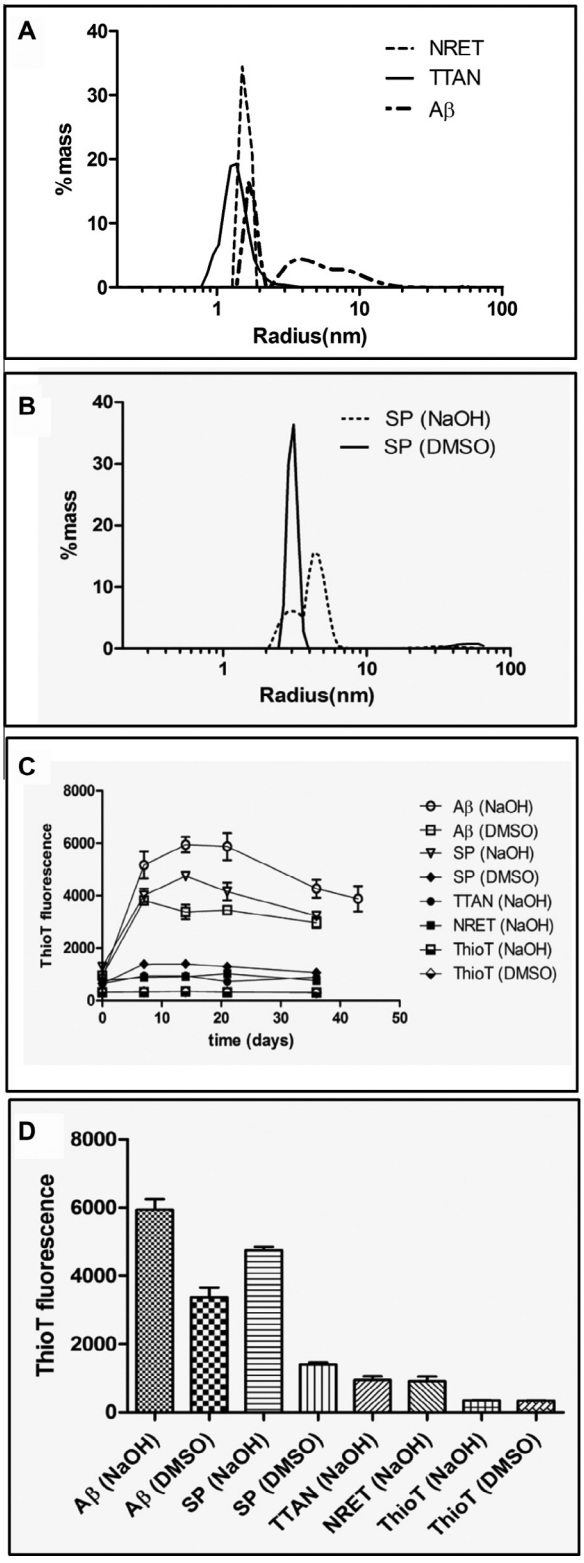

Fig. 2. DLS and ThT analysis of Aβ and mutants. DLS plots are representative of the average of 50 individual 5s DLS collections for 3 separate dilutions of (A) $A\beta_{42}$, $A\beta_{42}$TTAN and $A\beta_{42}$NRET pretreated with NH_4OH and dissolved in DMSO. (B) $A\beta_{42}$SP pretreated with both DMSO and NH_4OH. The $A\beta_{42}$TTAN, $A\beta_{42}$NRET, and $A\beta_{42}$SP prepared in DMSO appear as monomodal monodisperse whereas the $A\beta_{42}$ and $A\beta_{42}$SP prepared in NaOH are multimodal polydisperse. The extended ThT assay (C) show that $A\beta_{42}$TTAN, $A\beta_{42}$NRET made up in NaOH show little if no aggregation over 30 days as does $A\beta_{42}$SP made up in DMSO, whereas $A\beta_{42}$ in both DMSO and NaOH, and $A\beta_{42}$SP in NaOH exhibit aggregation peaking at day 14 (D).

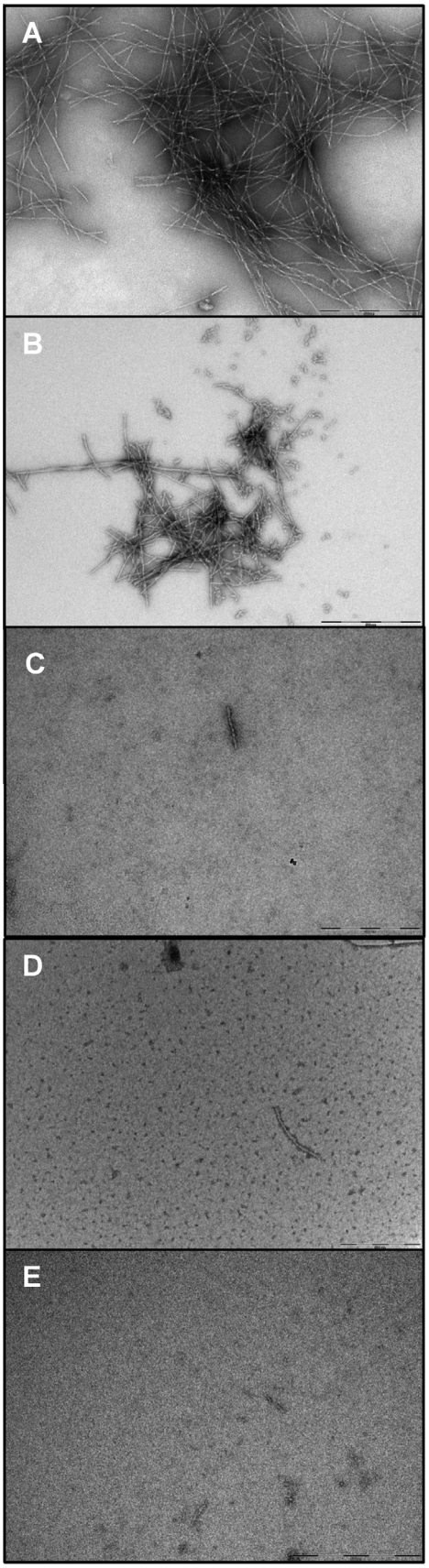

Fig. 3. TEM micrographs of Aβ and mutants. (A) $A\beta_{42}$ control; (B) $A\beta_{42}$SP; (C) $A\beta_{42}$TTAN; (D) $A\beta_{42}$NRET peptides were dissolved in 60 mM NaOH and allowed to fibrillise in PBS for 1 month at 37 °C. (E) $A\beta_{42}$SP dissolved in DMSO before dilution into phosphate buffer and fibrillisation as above.

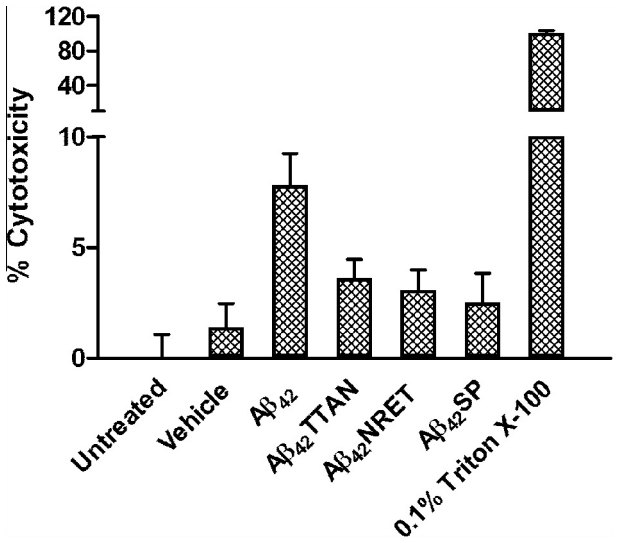

Fig. 4. Cell toxicity. PC-12 cultures treated with 15 μM of each peptide for 72 h, demonstrating that $A\beta_{42}$ is more cytotoxic than $A\beta_{42}$TTAN, $A\beta_{42}$NRET or $A\beta_{42}$SP. Triton X-100 is a cytotoxicity control.

cytotoxicity), $A\beta_{42}$ (15 μM) treatment increased cytotoxicity to 7.8 ± 1.5% (Fig. 4). Compared with $A\beta_{42}$, the cultures treated with $A\beta_{42}$TTAN, $A\beta_{42}$NRET and $A\beta_{42}$SP mutants had lower cytotoxicities of 3.6 ± 0.9%, 3.1 ± 0.9% and 2.5 ± 1.4%, respectively.

5. Discussion

The disaggregation or sequestration of Aβ oligomers and plaques may be a strategy for the treatment and prevention of AD. Thus, insight into the mechanisms of self-association has the capacity to inform and guide our design of future therapeutics. Based on our X-ray structural studies of the Aβ P3 fragment (residues 18–41) [10], as well as previous literature [17], we identified key hydrophobic residues at positions 19, 32, 34, 35, 39 and 41 as important in oligomer and amyloid formation. Utilising this information, we designed and produced three full length $A\beta_{42}$ peptides with mutations at these residues ($A\beta_{42}$TTAN, $A\beta_{42}$NRET, and $A\beta_{42}$SP) and compared their aggregation properties against wt $A\beta_{42}$. The Aβ peptide field has been criticised for lack of consistency in the reporting of peptide production and validation [27]. In our studies we have carefully stated the peptide preparation method (distinguishing DMSO from NaOH), to validate the solubilised peptides by GF and CD spectroscopy (see Supplementary Material) and to internally compare all peptides in parallel against a comprehensive series of assays. We discuss each of these aspects in turn.

5.1. Peptide preparation and comparison of DMSO or NaOH

Throughout this investigation, we utilised our established and consistent method of Aβ peptide preparation by NH_4OH pre-treatment followed by dissolving in NaOH. In contrast to the reported non-aggregating nature of $A\beta_{42}$SP [17], when pre-treated with NH_4OH it increased ThT fluorescence over time and correlated with observed short protofibrils and longer fibrils (though less fibrils compared with wt $A\beta_{42}$). In contrast with the immediate GF assay, aggregation in assays with longer incubation times (>24 h *i.e.* TEM and ThT) clearly showed the effect of dissolving $A\beta_{42}$SP in NaOH (as opposed to DMSO). Further supporting this data was the small amount of a higher molecular weight species for $A\beta_{42}$SP separated by GF. The original $A\beta_{42}$SP methodology [17] involved dissolving in DMSO or DMSO/NaOH before dilution into buffers. In that study, both DMSO and DMSO/NaOH were used. Similarly, $A\beta_{42}$ was also less aggregating in the ThT assay when prepared in DMSO. In contrast, the biophysical properties of $A\beta_{42}$TTAN and $A\beta_{42}$NRET did not differ when prepared in either NaOH or DMSO. Low levels of DMSO can significantly change peptide and protein properties and secondary structure by encouraging protein unfolding and denaturation [28]. Indeed, Shen et al. [29] showed that Aβ fibril formation is significantly affected by the solvent in which the Aβ peptide is prepared, a result supported by our observations. In contrast, the $A\beta_{42}$TTAN and $A\beta_{42}$NRET appear non-aggregating regardless of the solvent.

5.2. Peptide validation by gel filtration (GF) and CD spectrometry

Early stage aggregation can be measured by GF. Unlike wt $A\beta_{42}$, $A\beta_{42}$TTAN, $A\beta_{42}$NRET and $A\beta_{42}$SP are non-aggregating or slower aggregators because they each eluted as one peak of low oligomeric size, with little tendency to shift to higher molecular weight species within the short incubation period (30 min). Mutant peptides were studied using CD (Supplementary Material) to compare the secondary structure of native $A\beta_{42}$ with the mutant peptides over 24 h. Using freshly prepared aggregate free peptide preparations at both $t = 0$ and $t = 24$ h, the $A\beta_{42}$TTAN, $A\beta_{42}$NRET and $A\beta_{42}$SP all exhibited similar secondary structure revealing that the point mutations did not change the secondary structure compared to the wild type peptide.

5.3. Aggregation assays show Aβ42TTAN, Aβ42NRET to be non-associating

Our results clearly demonstrate that the mutants $A\beta_{42}$TTAN and $A\beta_{42}$NRET are non-aggregating in: (1) SDS–PAGE, where a single species for both mutants migrates at a similar size to that of monomeric $A\beta_{42}$, with no higher molecular weight SDS-resistant species. In contrast $A\beta_{42}$SP displays some higher order aggregates. (2) DLS. Here, R_h for wild type $A\beta_{42}$ monomer has been experimentally determined by fluorescence correlation spectroscopy (FCS) [30] in DMSO to be 0.9 ± 0.1 nm, in agreement with previous R_h calculated by *in silico* studies [31,32]. In this study, $A\beta_{42}$NRET appears as a single species with a slightly larger radius than that observed for monomeric, whereas $A\beta_{42}$TTAN also has a larger R_h, as well as exhibiting a slightly broader peak and may also indicate more than a single species. It seems that these non-single species are stabilized at the R_h range of <2.0 nm which includes the R_h estimate of ~1.7 nm for tetrameric form of $A\beta_{17-41}$ [10]. In contrast, $A\beta_{42}$SP shows some aggregation along the pathway towards fibrillisation observed for the wt. (3) ThT assay, where neither $A\beta_{42}$TTAN nor $A\beta_{42}$NRET showed significant fluorescence increase, compared to wt, and to a lesser extent $A\beta_{42}$SP, as detailed above. (4) TEM. Analysis of aged peptides shows that the $A\beta_{42}$ forms extensive masses of fibrils whilst the $A\beta_{42}$TTAN remains essentially soluble with only the occasional clump of protofibrils detected. Short single fibrils of $A\beta_{42}$NRET dissolved in NaOH were observed in less than 1% of the fields.

5.4. Effect of residue substitution

The biophysical properties described above are correlated with a weaker level of cytotoxicity in a neuronal cell model. The interaction of $A\beta_{40}$ with neuronal cells initially involves binding to the cell membrane within minutes [33,34]. It is beyond the scope of this study to determine whether the reduced cytotoxicity with $A\beta_{42}$TTAN, $A\beta_{42}$NRET and $A\beta_{42}$SP mutants is due to aggregation state or reduced affinity for the cell membrane. It is speculated that the lack of aggregation results in an oligomeric complex that is unable to penetrate the membrane, or specifically interact with

neuronal receptors or both [33,34]. Our identification of a series of residues in the C-terminal region 32–42 of Aβ, based on structural predictions, emphasises the importance of this region in Aβ aggregation and neurotoxicity and provides a strategy for the design of future therapeutic peptides or compounds towards amelioration of protein folding disorders.

Acknowledgments

The authors would like to thank Dr. Shane Seabrook for assistance with the DLS measurements and Mr Nick Bartone for assistance with mass spectrometry. This work was supported by the CSIRO Preventative Health Flagship and CRC for Mental Health.

Appendix A. Supplementary data

Supplementary data associated with this article can be found, in the online version, at http://dx.doi.org/10.1016/j.bbrc.2014.09.102.

References

[1] H.W. Querfurth, F.M. LaFerla, Alzheimer's disease, N. Engl. J. Med. 362 (2010) 329–344.
[2] M.D. Kirkitadze, G. Bitan, D.B. Teplow, Paradigm shifts in Alzheimer's disease and other neurodegenerative disorders: the emerging role of oligomeric assemblies, J. Neurosci. Res. 69 (2002) 567–577.
[3] P.N. Lacor, M.C. Buniel, L. Chang, S.J. Fernandez, Y. Gong, K.L. Viola, M.P. Lambert, P.T. Velasco, E.H. Bigio, C.E. Finch, G.A. Krafft, W.L. Klein, Synaptic targeting by Alzheimer's-related amyloid beta oligomers, J. Neurosci. 24 (2004) 10191–10200.
[4] L.F. Lue, Y.M. Kuo, A.E. Roher, L. Brachova, Y. Shen, L. Sue, T. Beach, J.H. Kurth, R.E. Rydel, J. Rogers, Soluble amyloid beta peptide concentration as a predictor of synaptic change in Alzheimer's disease, Am. J. Pathol. 155 (1999) 853–862.
[5] Y. Gong, L. Chang, K.L. Viola, P.N. Lacor, M.P. Lambert, C.E. Finch, G.A. Krafft, W.L. Klein, Alzheimer's disease-affected brain: presence of oligomeric A beta ligands (ADDLs) suggests a molecular basis for reversible memory loss, Proc. Natl. Acad. Sci. U.S.A. 100 (2003) 10417–10422.
[6] J.P. Cleary, D.M. Walsh, J.J. Hofmeister, G.M. Shankar, M.A. Kuskowski, D.J. Selkoe, K.H. Ashe, Natural oligomers of the amyloid-beta protein specifically disrupt cognitive function, Nat. Neurosci. 8 (2005) 79–84.
[7] C. Hureau, P. Faller, Abeta-mediated ROS production by Cu ions: structural insights, mechanisms and relevance to Alzheimer's disease, Biochimie 91 (2009) 1212–1217.
[8] G. Perry, L.M. Sayre, C.S. Atwood, R.J. Castellani, A.D. Cash, C.A. Rottkamp, M.A. Smith, The role of iron and copper in the aetiology of neurodegenerative disorders: therapeutic implications, CNS Drugs 16 (2002) 339–352.
[9] S. Jawhar, O. Wirths, T.A. Bayer, Pyroglutamate amyloid-beta (Abeta): a hatchet man in Alzheimer disease, J. Biol. Chem. 286 (2011) 38825–38832.
[10] V.A. Streltsov, J.N. Varghese, C.L. Masters, S.D. Nuttall, Crystal structure of the amyloid-beta p3 fragment provides a model for oligomer formation in Alzheimer's disease, J. Neurosci. 31 (2011) 1419–1426.
[11] Y. Shen, A. Joachimiak, M.R. Rosner, W.J. Tang, Structures of human insulin-degrading enzyme reveal a new substrate recognition mechanism, Nature 443 (2006) 870–874.
[12] A.S. Gardberg, L.T. Dice, S. Ou, R.L. Rich, E. Helmbrecht, J. Ko, R. Wetzel, D.G. Myszka, P.H. Patterson, C. Dealwis, Molecular basis for passive immunotherapy of Alzheimer's disease, Proc. Natl. Acad. Sci. U.S.A. 104 (2007) 15659–15664.
[13] L.A. Miles, K.S. Wun, G.A. Crespi, M.T. Fodero-Tavoletti, D. Galatis, C.J. Bagley, K. Beyreuther, C.L. Masters, R. Cappai, W.J. McKinstry, K.J. Barnham, M.W. Parker, Amyloid-beta-anti-amyloid-beta complex structure reveals an extended conformation in the immunodominant B-cell epitope, J. Mol. Biol. 377 (2008) 181–192.
[14] K. Takano, S. Endo, A. Mukaiyama, H. Chon, H. Matsumura, Y. Koga, S. Kanaya, Structure of amyloid beta fragments in aqueous environments, FEBS J. 273 (2006) 150–158.
[15] L. Yu, R. Edalji, J.E. Harlan, T.F. Holzman, A.P. Lopez, B. Labkovsky, H. Hillen, S. Barghorn, U. Ebert, P.L. Richardson, L. Miesbauer, L. Solomon, D. Bartley, K. Walter, R.W. Johnson, P.J. Hajduk, E.T. Olejniczak, Structural characterization of a soluble amyloid beta-peptide oligomer, Biochemistry 48 (2009) 1870–1877.
[16] R.M. Nisbet, S.D. Nuttall, R. Robert, J.M. Caine, O. Dolezal, M. Hattarki, L.A. Pearce, N. Davydova, C.L. Masters, J.N. Varghese, V.A. Streltsov, Structural studies of the tethered N-terminus of the Alzheimer's disease amyloid-beta peptide, Proteins 81 (2013) 1748–1758.
[17] C. Wurth, N.K. Guimard, M.H. Hecht, Mutations that reduce aggregation of the Alzheimer's Abeta42 peptide: an unbiased search for the sequence determinants of Abeta amyloidogenesis, J. Mol. Biol. 319 (2002) 1279–1290.
[18] Q.I. Churches, J. Caine, K. Cavanagh, V.C. Epa, L. Waddington, C.E. Tranberg, A.G. Meyer, J.N. Varghese, V. Streltsov, P.J. Duggan, Naturally occurring polyphenolic inhibitors of amyloid beta aggregation, Bioorg. Med. Chem. Lett. 24 (2014) 3108–3112.
[19] E. Socher, H. Sticht, A.H. Horn, The conformational stability of nonfibrillar amyloid-beta peptide oligomers critically depends on the C-terminal peptide length, ACS Chem. Neurosci. 5 (2014) 161–167.
[20] C. Peters, E.J. Fernandez-Perez, C.F. Burgos, M.P. Espinoza, C. Castillo, J.C. Urrutia, V.A. Streltsov, C. Opazo, L.G. Aguayo, Inhibition of amyloid beta-induced synaptotoxicity by a pentapeptide derived from the glycine zipper region of the neurotoxic peptide, Neurobiol. Aging 34 (2013) 2805–2814.
[21] E.A. Fradinger, B.H. Monien, B. Urbanc, A. Lomakin, M. Tan, H. Li, S.M. Spring, M.M. Condron, L. Cruz, C.W. Xie, G.B. Benedek, G. Bitan, C-terminal peptides coassemble into Abeta42 oligomers and protect neurons against Abeta42-induced neurotoxicity, Proc. Natl. Acad. Sci. U.S.A. 105 (2008) 14175–14180.
[22] Schrodinger, LLC, The PyMOL Molecular Graphics System, Version 1.3r1, 2010.
[23] T.M. Ryan, J. Caine, H.D. Mertens, N. Kirby, J. Nigro, K. Breheney, L.J. Waddington, V.A. Streltsov, C. Curtain, C.L. Masters, B.R. Roberts, Ammonium hydroxide treatment of Abeta produces an aggregate free solution suitable for biophysical and cell culture characterization, PeerJ 1 (2013) e73.
[24] H. LeVine 3rd, Thioflavine T interaction with synthetic Alzheimer's disease beta-amyloid peptides: detection of amyloid aggregation in solution, Protein Sci. 2 (1993) 404–410.
[25] R.M. Nisbet, J. Nigro, K. Breheney, J. Caine, M.K. Hattarki, S.D. Nuttall, Central amyloid-beta-specific single chain variable fragment ameliorates Abeta aggregation and neurotoxicity, Protein Eng. Des. Sel. 26 (2013) 571–580.
[26] B.J. Kuipers, H. Gruppen, Prediction of molar extinction coefficients of proteins and peptides using UV absorption of the constituent amino acids at 214 nm to enable quantitative reverse phase high-performance liquid chromatography–mass spectrometry analysis, J. Agric. Food Chem. 55 (2007) 5445–5451.
[27] State of aggregation, Nat. Neurosci. 14 (2011) 399.
[28] A. Tjernberg, N. Markova, W.J. Griffiths, D. Hallen, DMSO-related effects in protein characterization, J. Biomol. Screen. 11 (2006) 131–137.
[29] C.L. Shen, R.M. Murphy, Solvent effects on self-assembly of beta-amyloid peptide, Biophys. J. 69 (1995) 640–651.
[30] S. Nag, B. Sarkar, A. Bandyopadhyay, B. Sahoo, V.K. Sreenivasan, M. Kombrabail, C. Muralidharan, S. Maiti, Nature of the amyloid-beta monomer and the monomer-oligomer equilibrium, J. Biol. Chem. 286 (2011) 13827–13833.
[31] N.G. Sgourakis, Y. Yan, S.A. McCallum, C. Wang, A.E. Garcia, The Alzheimer's peptides Abeta40 and 42 adopt distinct conformations in water: a combined MD/NMR study, J. Mol. Biol. 368 (2007) 1448–1457.
[32] A. Baumketner, S.L. Bernstein, T. Wyttenbach, G. Bitan, D.B. Teplow, M.T. Bowers, J.E. Shea, Amyloid beta-protein monomer structure: a computational and experimental study, Protein Sci. 15 (2006) 420–428.
[33] R.D. Johnson, J.A. Schauerte, K.C. Wisser, A. Gafni, D.G. Steel, Direct observation of single amyloid-beta(1–40) oligomers on live cells: binding and growth at physiological concentrations, PLoS One 6 (2011) e23970.
[34] H. Decker, K.Y. Lo, S.M. Unger, S.T. Ferreira, M.A. Silverman, Amyloid-beta peptide oligomers disrupt axonal transport through an NMDA receptor-dependent mechanism that is mediated by glycogen synthase kinase 3beta in primary cultured hippocampal neurons, J. Neurosci. 30 (2010) 9166–9171.